Geoderma 237–238 (2015) 88–97

Contents lists available at ScienceDirect

Geoderma

journal homepage: www.elsevier.com/locate/geoderma

Distinguishing and mapping permanent and reversible paludified landscapes in Canadian black spruce forests

Ahmed Laamrani [a,b,*], Osvaldo Valeria [a,b], Yves Bergeron [a,b], Nicole Fenton [a,b], Li Zhen Cheng [a,c]

[a] Université du Québec en Abitibi-Témiscamingue (UQAT), 445 boul. de l'Université, Rouyn-Noranda, Québec J9X 5E4, Canada
[b] Institut de recherche sur les forêts (IRF), Québec, Canada
[c] Institut de recherche en mines et en environnement (IRME), Québec, Canada

ARTICLE INFO

Article history:
Received 11 June 2014
Received in revised form 20 August 2014
Accepted 24 August 2014
Available online xxxx

Keywords:
Organic layer thickness
Clay Belt
Topographic wetness index
Topographic position index
Digital terrain model
Automated classification
LiDAR

ABSTRACT

Northern Canadian boreal forest is characterised by accumulation of a thick organic soil layer (paludification). Two types of paludification are recognised on the basis of topography and time since the last fire, viz., permanent paludification that dominates in natural depressions within the landscape, and reversible paludification that occurs on flat or sloping terrain over time following fire or mechanical site preparation. Accurate information about the occurrence of permanent or reversible paludification is required for land resource management. Such information is useful for the identification of locations of existing paludified areas where investment after harvesting should help to achieve greater productivity. This study investigated the potential for using a semi-automated method that was based on geomorphological analysis to map and differentiate between the two paludification types at the landscape scale within the Canadian Clay Belt region. For the purposes of this study, slope, topographic position index (TPI), and topographic wetness index (TWI) were generated from a LiDAR digital terrain model. TPI and TWI are, respectively, predictors of surface morphology (i.e., depressions vs flat areas) and moisture conditions (i.e., wet vs dry), and were used to explain paludification occurrence. A semi-automated classification method based on TPI and slope was firstly used to create six initial topographic position classes: deep-depressions, lower-slope depressions, flat surfaces, mid-slopes, upper-slopes, and hilltops. Each of these six classes was then combined with TWI classes (representing moisture conditions: wet, moderately wet, and dry) and this combination assisted in assigning each resulting class to one of the two paludification types. Slope and TWI values were used in sub-dividing the lower slope depression class, based on slope, into significantly different sub-classes, namely open and closed depressions (Tukey's HSD, $P < 0.001$). The distribution of field data (e.g., tree basal area, organic layer and fibric horizon thicknesses) within each position class provided additional information for corroborating the assignment of each class to a defined paludification type. The proposed semi-automated classification provided a relatively simple and practical tool for distinguishing and mapping permanent and reversible paludification types with an overall accuracy of 74%. The tool would be particularly useful for implementing strategies of sustainable management in remote boreal areas where field survey information is limited.

1. Introduction

Gradual accumulation of thick organic soil layers characterises boreal forest floors of the Hudson Bay–James Bay lowlands (Canada). Accumulations are attributed mainly to paludification, which generally creates wetter conditions that decrease soil temperature, decomposition rates, microbial activity, nutrient availability, and increase canopy openings (Crawford et al., 2003; Lavoie et al., 2005). Paludification can cause substantial productivity losses in the boreal forest and, consequently, potential sources of wood fibre. Paludification is especially problematic in the forested landscapes of the Clay Belt (Fig. 1A), a region within the Hudson Bay–James Bay lowlands, where it has facilitated the transformation of productive forests into unproductive forested peatlands. Within the Clay Belt, ground surface topography and time-since-last fire are two major drivers of paludification (Fenton et al., 2009). Consequently, two types of paludification (i.e., permanent and reversible) are recognised on the basis of these two factors. Theoretically, these two types occur in different locations across the landscape. Permanent paludification dominates in natural depressions, which have wetter soil conditions favouring organic layer build-up. Reversible paludification occurs on flat or sloping terrain, where feather moss-dominated ground cover is replaced by *Sphagnum* spp. (Fenton and Bergeron, 2006), after about 100 years following fire (Simard et al., 2007). Reversible paludification may be reversed through natural severe fire or a combination of silvicultural practices and site preparation,

* Corresponding author.
E-mail address: Ahmed.Laamrani@uqat.ca (A. Laamrani).

http://dx.doi.org/10.1016/j.geoderma.2014.08.011
0016-7061/

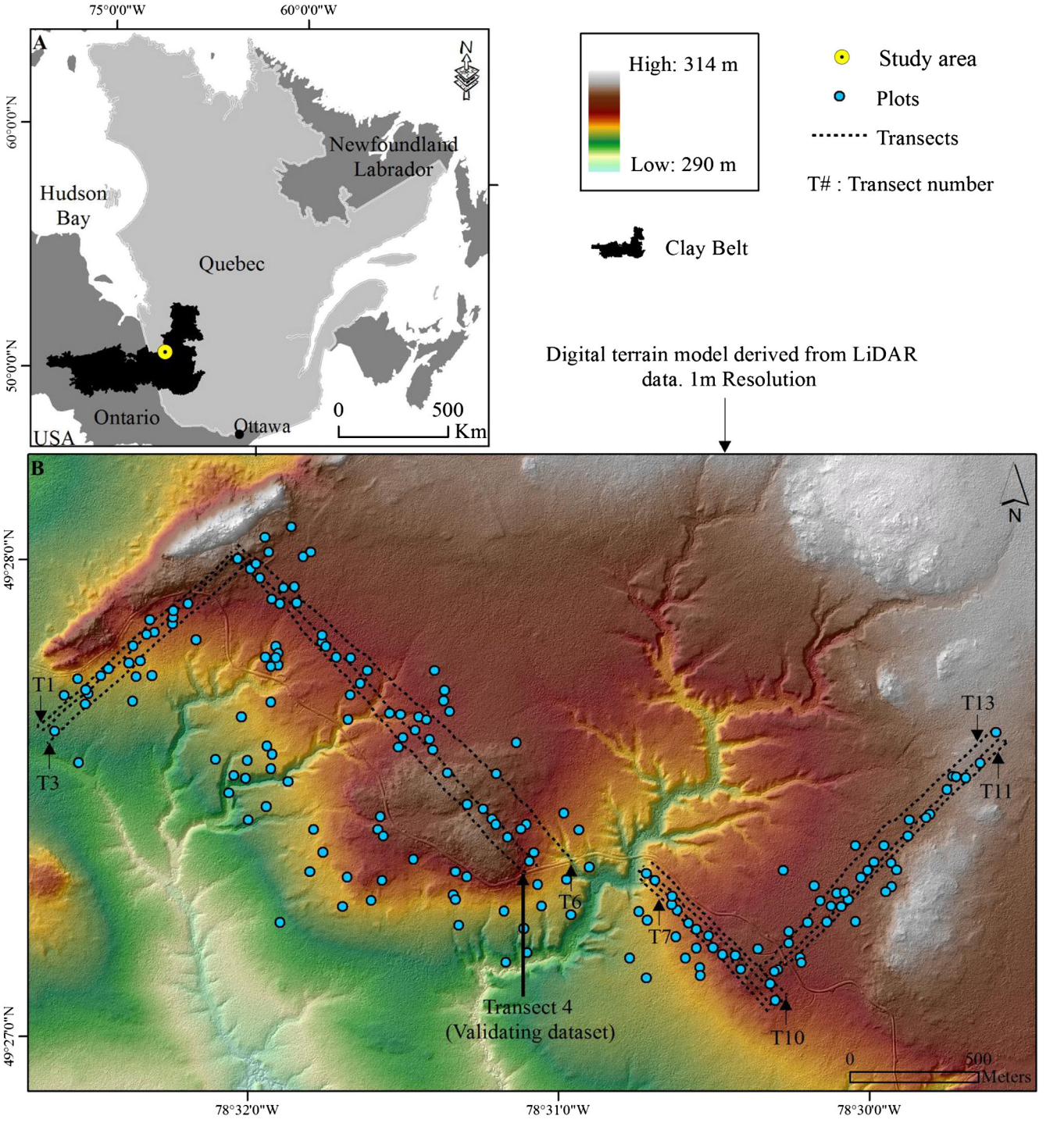

Fig. 1. Study location within the Clay Belt region of Ontario and Quebec (A). Topographic overview of the study area showing field sampling points along transects and plots (B).

as detailed by Fenton et al. (2009). In contrast, permanent paludification is not reversible, as its name suggests.

Several studies have dealt with either one or the other paludification type within Clay Belt black spruce (*Picea mariana* [Miller] BSP) forests (Fenton et al., 2005; Lavoie et al., 2005; Simard et al., 2009). Yet research examining spatial distributions of these two paludification types across larger areas is rare (Laamrani et al., 2014b,c; Lavoie et al., 2007). Mapping their occurrence at the landscape scale is critically important for land managers and decision-makers, if they are to implement appropriate management practices. To effectively manage black spruce forests in the Clay Belt, accurate spatial maps that can identify the two paludification types are required. Such maps could be used to delineate areas where efforts and investments should be made to achieve higher productivity after logging or to identify retention areas that maintain structural attributes and habitats. Finding the terrain attribute that can most easily differentiate between paludification types could be considered and addressed within the context of landscape classification.

Light Detection and Ranging (LIDAR, remote sensing system) is a practical technology for landscape analysis (Southee et al., 2012) and captures topographic features with high vertical and horizontal precision, making it suitable for this study. Also, LiDAR potentially provides information on surface morphology (e.g., flat areas vs depressions) and wetness conditions (e.g., wet vs dry), which are intuitively important in discriminating between reversible and permanent paludifications

(Laamrani et al., 2014b). The application of such indices is a powerful approach for landscape classification in forested environments (Emili et al., 2006; Laamrani et al., 2014b; MacMillan et al., 2007; Tchir et al., 2004).

While numerous methods and algorithms have been devised to classify the landscape into morphological classes (e.g., Clark et al., 2009; Creed and Beall, 2009; Lindsay and Creed, 2005), the majority of them have been developed largely for non-forestry applications (e.g., hydrology) and, in most cases, have not addressed characterisation of depressions in relatively flat or low relief areas. In the few studies attempting to distinguish depressions from other landscape classes (i.e., flats vs depressions; Lindsay and Creed, 2005), the approaches and algorithms that were used were complicated and very time-consuming; moreover, their implementation and interpretation frequently requires a solid statistical background. To avoid these issues and ultimately allow this technique to be applied by resource managers, our method had to be simple to implement, automated or semi-automated, compatible with GIS environments, and applicable to other areas. The objective of this study was to investigate the potential for using a semi-automated landscape classification method based on selected topographic indices to distinguish and map reversible and permanent paludified landscapes in Clay Belt black spruce forests.

2. Materials and Methods

2.1. Study Area

The study was located in the western black spruce-feather moss bioclimatic domain (Robitaille and Saucier, 1998), and more precisely, within the Clay Belt, a vast conifer-dominated region spanning the Ontario–Quebec border (Fig. 1a). The dominant landforms are flat plains, which were generated by extensive and thick glacio-lacustrine clay deposits that were left behind by pro-glacial Lake Ojibway (Veillette, 1994). Bedrock outcrops and gentle hills are also found within the Clay Belt. Our sampling site covered 720 ha of boreal forest, in which the elevation ranged from 290 m to 314 m, averaging 304 m above sea level. Ground surface slope ranged from 0 to 34%; about 65% of the area had slopes $\leq 3\%$, whereas slopes $\geq 16\%$ represented about 1% of the area. Drainage courses run locally in a southwestern direction through the study area to produce a relatively complex topography (Fig. 1b). Mean annual temperature is −0.7 °C and total annual precipitation is 906 mm (Environment Canada, 2011; Matagami weather station, about 60 km NE of the study area).

Black spruce dominates stands in the study area, whereas occasional stands dominated by jack pine (*Pinus banksiana* Lambert) or trembling aspen (*Populus tremuloides* Michaux) are dispersed across the landscape. Ground cover includes *Sphagnum* spp., feather mosses (principally *Pleurozium schreberi* (Brid.) Mitten) and shrubs (dwarf ericaceous species), which have variable coverage across the landscape.

2.2. Field Dataset Collection

Field data were collected during summer 2010 along transects, and within circular plots (Fig. 1b). At each sampling point along transects, organic layer thickness (OLT) was measured with an auger, following Laamrani et al. (2014a). One hundred and seventy-eight plots (400 m^2) were randomly distributed between and outside of transects; these included different forest types and topographic positions. In each plot, a pit was dug, and OLT and thickness of the fibric soil horizon were recorded. All trees that were larger than 9 cm in diameter at breast height (dbh; 1.3 m above ground level, which is considered to be the minimum merchantable limit) were recorded within each plot and used to calculate basal area (m^2/ha) as a productivity indicator. Overall, the field dataset consisted of three groups that were used for: topography/organic layer–terrain relationships (1380 points, corresponding to 10 m-interval sampling points along transects); vegetation/soil–terrain relationships (178 point-plots); and for validating predictive maps (170 points; transect #4; randomly selected).

2.3. Digital Terrain Model and Derived Topographic Variables

LiDAR data were collected on 28 May 2010 over 100 km^2 with a density of 2.8 points/m^2 and vertical accuracy RMSE of 0.065 cm. Raw LiDAR data (provided in LAS format) were pre-processed by separating canopy pulse returns from ground pulse returns. The last returns that were classified as ground surface were interpolated with 0.5 m resolution and gridded at a 10 m resolution to produce a digital terrain model (DTM). The DTM was principally used to identify topographic features at the landscape scale; we considered a 10 m grid resolution as adequately representing those features and capturing the area's topography (Laamrani et al., 2014a). Using standard procedures in ArcGIS 10 (ESRI, 2011), slope, elevation, topographic position index (TPI), and topographic wetness index (TWI) grids were created from DTM. In this study we employed LiDAR-generated TPI and TWI because we assume these are closely associated with permanent and reversible paludification mapping. Field sample locations were superimposed upon these grids, and corresponding parameters (topographic variables, field data information) were extracted for each sampling location. All field-sampling locations were recorded using GNSS (Global Navigation R8 Satellite System) with mm/cm-level accuracy to allow their direct comparison with the DTM.

2.3.1. TPI and Classification

TPI is the difference between a central cell elevation value and the average elevation of the neighbourhood around that cell. Neighbourhood refers to all grid cells, the centres of which lie within a defined radius of the central cell. Negative TPI indicates that the central cell is lower than its surroundings, while positive TPI means that it is higher than its average surroundings. TPI values of zero and near-zero indicate that the central cell is close to the mean elevation of the neighbourhood (Jenness et al., 2011; Weiss, 2001). Since TPI represents a measure of surface morphology (Tagil and Jenness, 2008), its values potentially provide a simple and powerful means of classifying the landscape into topographic position classes. First, we used Weiss's method to classify the landscape into discrete topographic position classes using the standard deviations of TPI and slope (Fig. 2a). Second, we enriched Weiss's classification with new classes described in Section 3. Weiss's classification criteria details are provided in Table 1.

2.3.2. TWI and Surface Water Movement

TWI is a relative measure of soil moisture for a specific cell and is regarded both as an indicator of topographically driven soil surface water distribution (Beven and Kirkby, 1979; Wilson and Gallant, 2000), and as a guide to water movement within a particular landscape (McKenzie and Ryan, 1999). TWI values were calculated for each cell (10 m × 10 m) using the formula $TWI = \ln(As / \tan\beta)$ (Moore et al., 1993), where As is the specific catchment area and β is the local slope angle (degrees). Highest values of TWI were associated with wet areas, while the lowest TWIs were associated with dry areas (Bou Kheir et al., 2010; Sørensen et al., 2006).

2.4. Assignment of Paludification Types to Topographic Position Classes and Their Validation

Assignment of paludification types to a topographic position class based on the relationship between soil wetness classes and the six topographic position classes was realised in several steps:

First, standard deviations of TPI values and slope were used to classify the landscape into six topographic position classes that were denoted: deep depressions, lower slope depressions, flat surfaces, mid-slopes, upper slopes, and hilltops (Fig. 3). The six classes were generated using Weiss's classification criteria and the *Land Facet Corridor Tools* ArcGIS

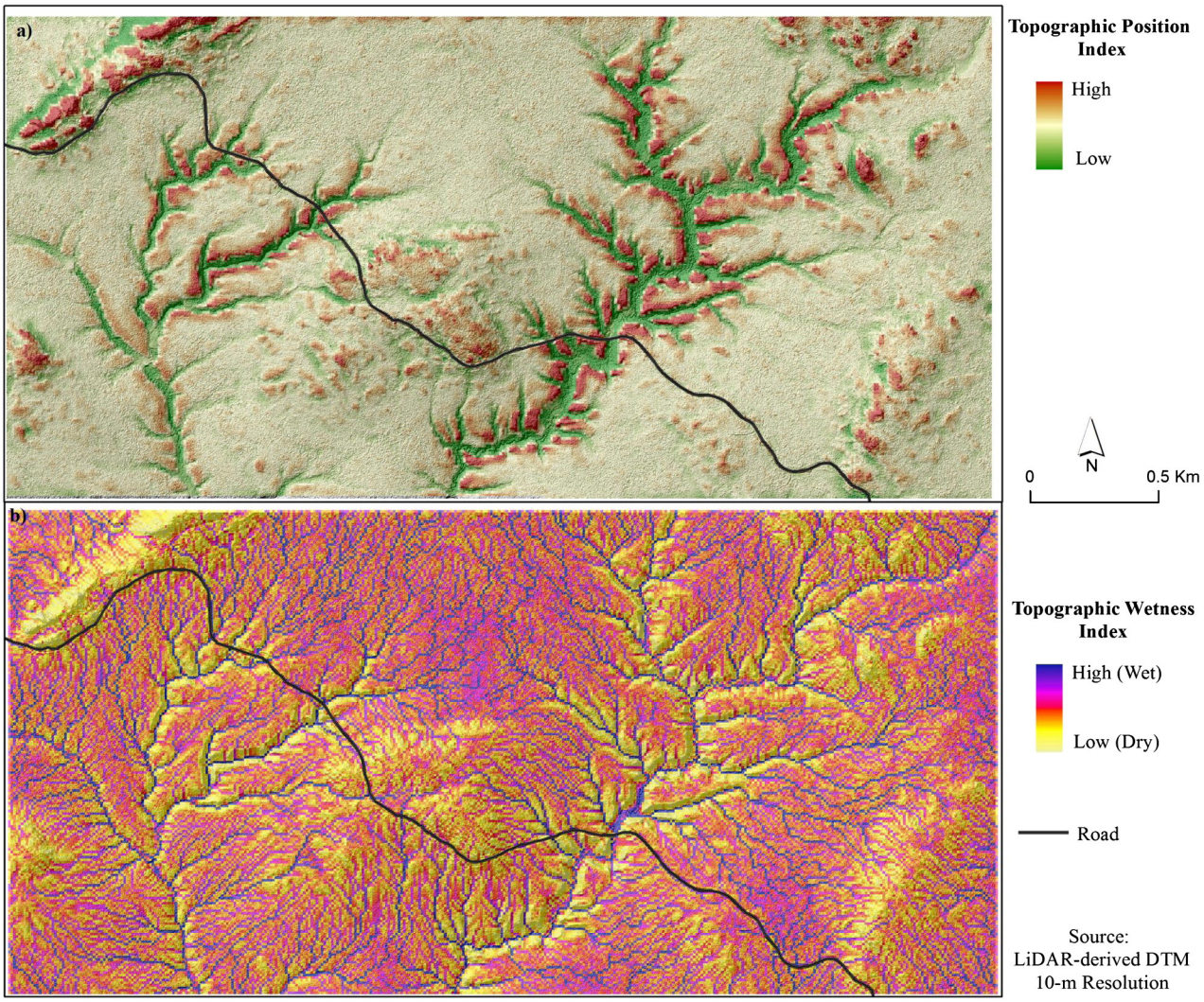

Fig. 2. TPI and TWI grids used in this study. (a) The highest and lowest TPI values occur in higher and lower terrain positions, respectively. (b) The lowest, moderate, and highest TWI values are found in dry, moderately wet, and wet areas, respectively.

extension (Jenness et al., 2011). In following Weiss's scheme, high TPI values were found at higher terrain positions (e.g., hilltops), while low TPI values were found in lower terrain positions (e.g., depressions). As shown by other studies (e.g., Deumlich et al., 2010), the choice of neighbourhood size was based on an iterative process in which several circular neighbourhood sizes were tried until the output that best corresponded with actual study area topography was generated (50 m-radius in our case; Fig. 2a).

Table 1
Descriptions of six topographic position classes based on standardised topographic position index (TPI) and slope.

Topographic position classes		Criteria		Area[b]	
Class[a]	Description[b]	TPI[a]	Slope (%)[b]	ha	(%)
1	Deep depressions	TPI ≤ −1 SD		43	6
2	Lower slope depressions	−1 SD < TPI ≤ −0.5 SD		74	10
3	Flat surfaces	−0.5 SD < TPI < 0.5 SD	≤1.8	385	53
4	Mid-slopes	−0.5 SD < TPI < 0.5 SD	>1.8	88	12
5	Upper-slopes	0.5 < SD TPI ≤ 1		92	13
6	Hilltops	TPI > 1 SD		39	5

Note: TPI and slope criteria follow Weiss (2001) and Laamrani et al. (2013b), respectively.
[a] Designation according to Weiss' classification scheme.
[b] Designation according to this study. SD = Standard Deviation.

Second, soil wetness classes were then created by classifying TWI values (Fig. 2b) into three categories of wetness (wet, moderately wet, dry), using the same TWI thresholds that were determined by Laamrani et al. (2014b; i.e., TWI threshold of 7). These thresholds were similar to values that were reported elsewhere to delineate wet areas (e.g., 6.9 TWI threshold, reported by Creed and Sass, 2011). We then analysed TWI class distributions within each topographic position class. Combinations of TWI classes and topographic position classes produced a set of new categories (e.g., dry/flat surfaces, wet/flat surfaces, and dry/upper).

Third, each of these new classes was assigned to a defined paludification type, based on relationships between soil wetness classes, slope and the six topographic position classes. To do so, we used a decision key procedure, which is similar to a non-parametric regression tree modelling approach. The decision key of the logic that was followed in assigning a topographic class to the paludification types is further detailed in the Results and Discussion section. For example, an area on the landscape with the dry/upper combination may reasonably be assigned to the reversible paludification type. Field data (vegetation and soil) were also used to determine whether the assignment of topographic position class to one or the other paludification type was plausible, together with the ease with which a paludified area could be reversed. For example, paludified areas with lower OLT and dry

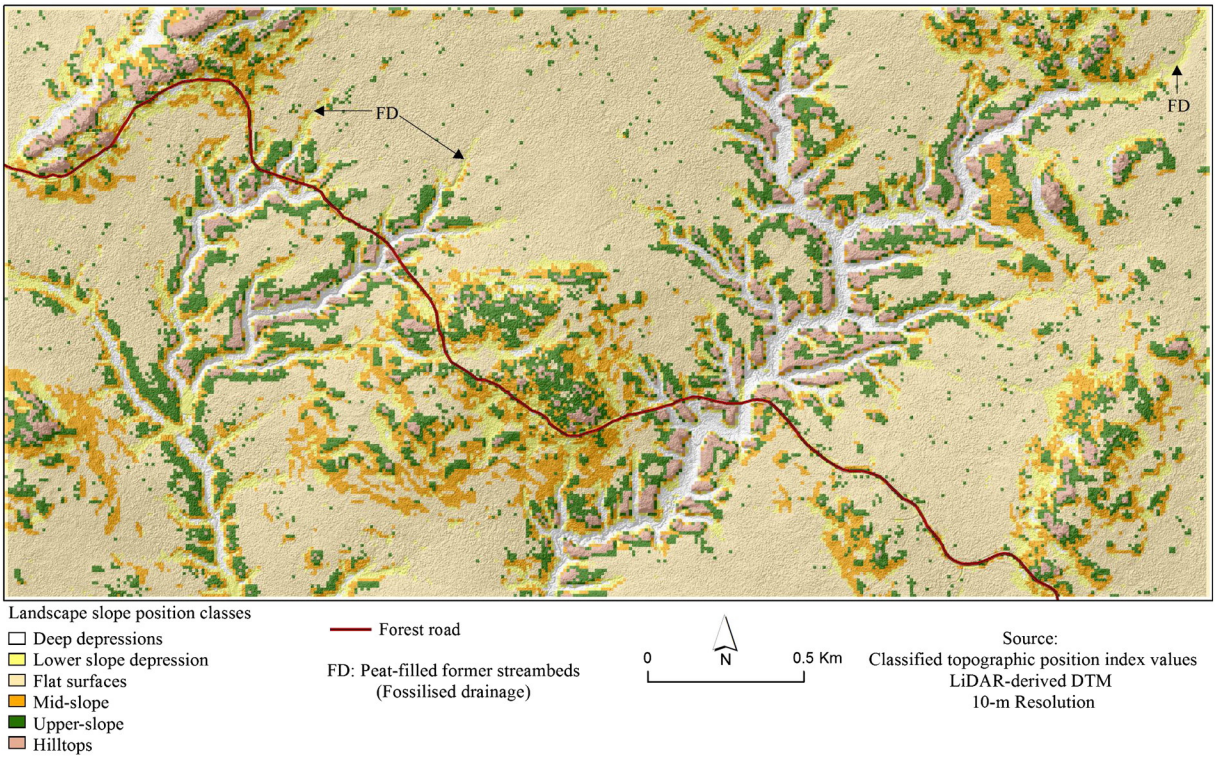

Fig. 3. Thematic landscape map based on TPI values. Descriptions of each class are in Table 1.

conditions would be much easier to reverse than those with higher OLT and wet conditions.

2.5. Statistical Analyses

Prior to statistical analysis, the issue of collinearity between TPI and TWI was addressed. To do so, we used the most commonly applied method, which uses a Pearson correlation coefficient threshold (|r|) of 0.7 as an approximate indicator (Dormann et al., 2013). An absolute value of r that exceeds 0.7 indicates highly correlated variables, and vice-versa. In our case, the two variables (TPI and TWI) were not strongly correlated, i.e., $|r| = 0.3$; therefore, the assumptions regarding the lack of collinearity between the two variables were satisfied.

Slope, elevation, TWI and field data statistics were computed within the resulting topographic position classes. One-way analysis of variance (ANOVA) tested equality of variable means among the resulting topographic classes. Post-hoc Tukey HSD tests of mean topographic indices and field responses separated pairs of topographic landscape classes. In other words, we classified space into initial six classes that were based on variables extracted from our DTM. Then, ANOVA analysis and post-hoc means tests were used to confirm or refute significant class differences. Significance was declared at $\alpha = 0.05$, with all statistical analyses being performed in R (R Development Core Team, 2011).

3. Results and Discussion

3.1. Topographic Position Classification

Results of topographic position classification based on Weiss's criteria are summarised in Table 1, and spatial distributions of the six topographic position classes are shown in Fig. 3. More than 53% of the area was classified as flat surfaces, 6% as deep depressions, 10% as lower slope depressions, 12% as mid-slopes, 13% as upper-slopes, and 5% as hilltops. Flat surfaces and mid-slope areas had the same TPI thresholds (Table 1), with slope values being used to distinguish between these two possibilities. We used a 1.8% slope threshold based on our recent work, in which it was deemed appropriate for distinguishing areas with lower and higher slopes (Laamrani et al., 2014a). In using Weiss's method, other studies have similarly applied various slope threshold values to distinguish between flat and mid-slope areas (e.g., De Reu et al., 2013; Deumlich et al., 2010).

3.2. Relationship Between Topographic Position Classes and Terrain Attributes

Fig. 4 shows the relationships between cell-derived means of individual topographic variables that were used in this study and the six topographic position classes. As was confirmed by field surveys, greatest values (high wetness) were found in depressions (i.e., channels) in flat terrain, and in topographic hollows at higher elevation (i.e., local bedrock depressions). Mean TWI decreased with increasing local topographic relief, from deep depressions (10 ± 0.64; mean ± SE), through flat surfaces (9 ± 0.05), to hilltops (7 ± 0.16). Mean TWI significantly differed among classes (ANOVA, $P < 0.001$; Fig. 4), suggesting that it could be used as a complementary tool for further dividing slope positions within the landscape. Mean ground surface slopes and elevations varied significantly among topographic position classes (Fig. 4). Slope was lowest on flat surfaces ($2 \pm 0.03\%$), intermediate in lower slope depressions ($5 \pm 0.20\%$), and highest on hilltops ($6 \pm 0.58\%$). Upper-slope and hilltop classes did not differ (Tukey's HSD test, $P > 0.05$), but other classes significantly differed from one another (Tukey's HSD tests, $P < 0.05$; Fig. 4).

3.3. Assigning Topographic Position Classes to Paludification Types

Table 2 illustrates results of the assignment of each topographic position classes to the paludification types.

3.3.1. Deep Depression Class

Deep depressions (class 1) were frequently associated with deeper active streams and treeless depressions, and accurately recognised by Weiss's classification (75% site matching). About 67% of class 1 was

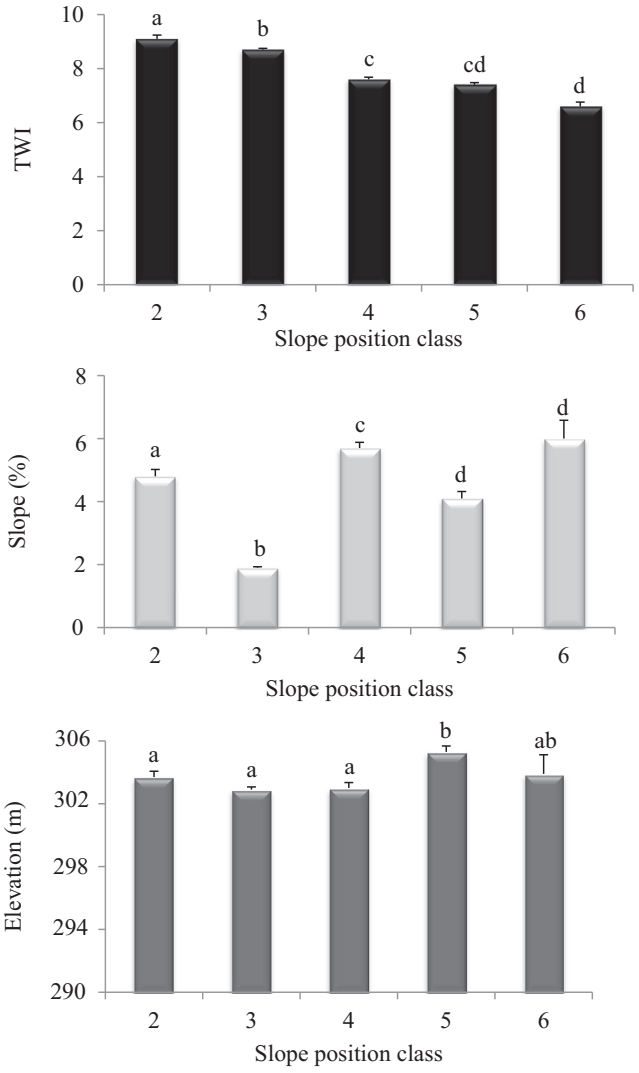

Fig. 4. Variation in TWI, slope, and elevation values within topographic position classes. Classes 2 to 6 (x-axis) refer to lower slope depressions, flat surfaces, mid-slopes, upper slopes, and hilltops, respectively. Error bars indicate SE of the mean; different letters designate statistically significant ($P < 0.05$) differences, according to pairwise Tukey tests.

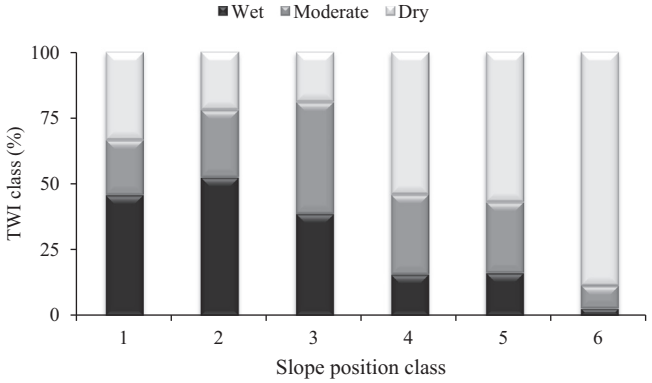

Fig. 5. Distribution of TWI classes within each of the six topographic position classes. Class numbers 1 to 6 are referred to in Fig. 4.

dominated by wet or moderately wet soils (Fig. 5). Since class 1 mostly represented permanently saturated or inundated areas, it was not considered important from a forest management perspective, and was deliberately excluded from our field survey and subsequent analyses.

3.3.2. Lower Slope Depression Class

Lower slope depressions (class 2) were frequently identified in shallow depressions (negative TPI), and associated with elongated, peat-filled former streambeds (fossilised drainage systems) and depressions within the underlying bedrock (Fig. 6; e.g., areas between positions 320 m and 360 m, and 1200 m and 1300 m). To our knowledge, this type of paludified depression has never been reported in the Canadian boreal forest and is rarely mentioned in the literature from other world regions (e.g., Gorozhankina, 1997). As is the case for class 1, wet and moderately wet soil predominated in the lower slope class (79%; Fig. 5).

Class 2 had a mean OLT of 38 ± 1.8 cm, mean tree basal area of 28 ± 3.1 m^2/ha (low productivity), and a mean fibric horizon thickness of 14 ± 2.5 cm (Table 2). For most variables that were used (topographic and field data), class 2 exhibited high standard errors (SE), suggesting that sub-division of the initially defined class was required. Reducing this variability within class 2 resulted in splitting lower slope depressions into two sub-classes (closed and open depressions), based upon a 1.8% slope threshold (Laamrani et al., 2014a). Once splitting was performed, the resulting open depressions exhibited greater mean tree basal area (39 ± 2.2 m^2/ha), lower OLT (29 ± 1.4 cm), and a more decomposed fibric horizon (thickness of 10 ± 1.9 cm) (Table 2). Closed

Table 2
Assignment of topographic position classes and sub-classes to paludification types and summary of field data (organic layer thickness "OLT" and basal area) that were used to corroborate this assignment.

Topographic position class			OLT (mean ± SE cm)		Basal area (mean ± SE m^2/ha)	Paludification type assignment	Producer's accuracy
#	Sub-class[a]	Description	Total	Fibric			
2		Lower slope depressions	38 ± 1.8	14 ± 2.5	28 ± 3.1		86%
	2.1	Closed depressions	53 ± 3.5	17 ± 5.0	18 ± 2.3	Permanent	80%
	2.2	Open depressions	29 ± 1.4	10 ± 1.9	39 ± 2.2	Reversible+++	91%
3		Flat surfaces	55 ± 0.9	15 ± 1.4	25 ± 1.3		87%
	3.1	Flat bogs	86 ± 2.4	35 ± 3.2	4.4 ± 1.1	Permanent	96%
	3.2	Flat moderate/wet surfaces	52 ± 1.3	14 ± 1.4	26 ± 2.8	Reversible+	N/A
	3.3	Flat dry surfaces	37 ± 2.0	10 ± 2.4	25 ± 1.2	Reversible++	N/A
4		Mid-slopes	29 ± 1.0	8 ± 1.0	31 ± 1.5	Reversible++++	62%
5		Upper-slopes	36 ± 1.3	8 ± 1.7	36 ± 2.3	Reversible+++	59%
6		Hilltops	26 ± 1.3	8 ± 1.9	35 ± 2.7	Reversible++++	57%
						Overall accuracy:	74%

N/A: accuracy not assessed because this sub-class division was based on soil wetness; no such field data were available.
Note: Overall accuracy is a ratio between correctly allocated number of field sites and the overall number of classified sites. Producer's accuracy measures classification accuracy for individual classes.
[a] Identified according to this study. SE = Standard Error. Plus (+) sign gradient refers to the ease with which a paludified area can be reversed (e.g., ++++ is easier than +++ and much easier than +).

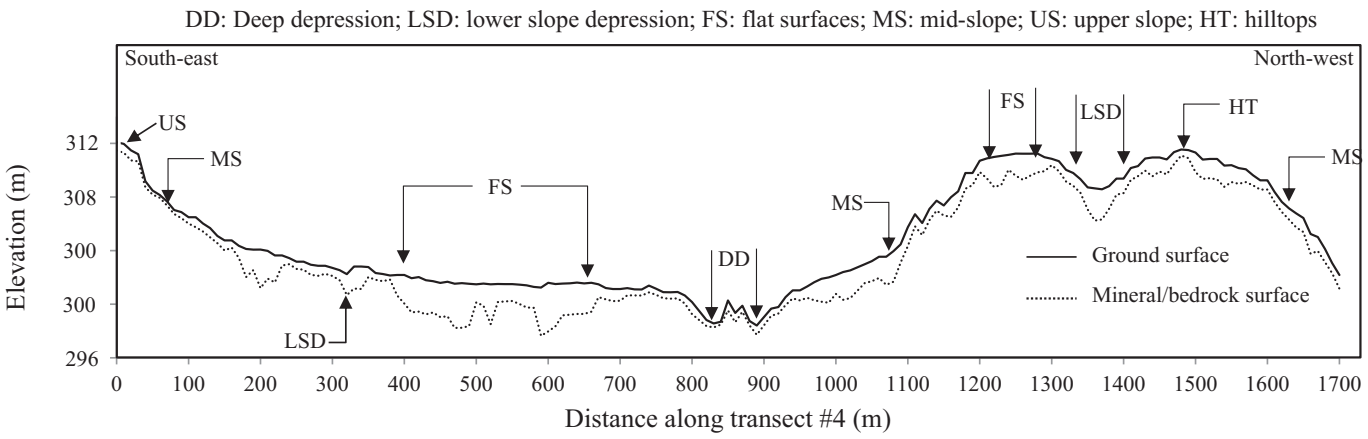

Fig. 6. Landscape profile section of the surface topography along transect #4. The distance between continuous and dashed curves represents OLT with vertical exaggeration of 3×.

depressions, in comparison, had lower tree basal areas (18 ± 2.3 m^2/ha), greater OLT (53 ± 3.5 cm), and greater fibric horizon thicknesses (17 ± 5.0 cm). Consequently, open and closed depression sub-classes significantly differed from one another (Tukey's HSD test, $P < 0.001$) with respect to the aforementioned variables.

The closed depressions class likely represent locations within the landscape with wetter soil conditions favouring organic layer accumulation, and where surface runoff is impeded or slowed down. Open depressions likely represent areas within the landscape with shallow organic layers, which are not closed to downslope water movement and are more favourable for tree growth. Distinctions between open and closed depressions were not initially captured by Weiss's classification, but they were easily added to it (Weiss' method) using a new slope criterion (open depression, slope > 1.8%; closed depression, slope ≤ 1.8%).

3.3.3. Flat Surface Class

Most of the area under study was classified as flat surfaces (class 3), not surprising given the predominance of flat ground (Veillette, 1994). About 81% of class 3 sites had moderately wet (39%) to wet (42%) soils (Fig. 5). Among initially defined classes, class 3 had the greatest OLT (55 ± 0.9 cm) and lowest tree basal areas (25 ± 1.3 m^2/ha; Table 2). Trees in class 3 plots exhibited a broad range of basal area (0.59–50.59 m^2/ha), suggesting that local sources of variation were not considered during landscape classification (e.g., the shape of the underlying material, time-since-last fire). Like class 2, class 3 variables (topography, vegetation, and soil) exhibited relatively high SE (Table 2), suggesting that flat surfaces could be split into more homogeneous subclasses. Indeed, field measurements showed that landscape locations corresponding to mineral soil depressions occurred mostly within flat bogs (Fig. 6; e.g., between positions 400 m and 650 m), with very low mean tree basal area (4.4 ± 1.1 m^2/ha), and very thick organic layers (86 ± 2.4 cm) and fibric horizons (35 ± 3.2 cm). These conditions seemed to be representative of permanent paludified areas that are not suited for forest management. While distinctions between two resulting subclasses were mainly based on field survey data, flat bog areas could be clearly recognised in forest inventory maps. When flat surfaces coinciding with depressions in mineral soil or bedrock were excluded from the initial dataset (non-split data), mean tree basal area increased slightly (27 ± 1.2 m^2/ha), while mean OLT (49 ± 2.7 cm) and fibric horizons decreased (13 ± 1 cm; Table 2).

Reduction in variability that was achieved by separating class 3 into two sub-classes using the shape of the underlying material was slightly less than that provided by Weiss's classification, suggesting that discriminating sub-classes was extremely difficult when based mainly on TPI; class 3 was located in flat areas where no slope variability in the terrain exists. Further sub-division of class 3 (excluding bogs) was based on TWI (dry, moderately wet, wet), which resulted in two new subclasses, i.e., flat moderate/wet surfaces and flat dry surfaces (Table 2; sub-classes 3.2 and 3.3, respectively). These new classes differed strongly in OLT (52 ± 1.3 cm and 37 ± 2.0 cm, respectively; Tukey's HSD, $P < 0.001$) but did not differ in terms of tree basal area (26 ± 2.8 m^2/ha vs 25 ± 1.2 m^2/ha; Tukey's HSD, $P = 0.95$). Time-since-fire could not be similarly used to reduce variability within the dataset; based on field observations, stands in the study area belonged to one of two age classes (75- and 125-years-old), where the first class was over-represented (89% of sample points) relative to the second (11%).

3.3.4. Mid-slope, Upper Slope and Hilltop Classes

Mid-slope (class 4), upper slope (class 5), and hilltop (class 6) classes were generally associated with upper terrain positions. The three classes included a high percentage of dry sites (54%, 57% and 89%, respectively; Fig. 5). As expected, these sloping surfaces (classes 4, 5, and 6) had relatively high tree basal areas (31 ± 1.5 m^2/ha, 36 ± 2.3 m^2/ha, and 35 ± 2.7 m^2/ha, respectively), and low/moderate OLTs (29 ± 1.0 cm, 36 ± 1.3 cm and 26 ± 1.3 cm, respectively; Table 2), most likely a result of their prevailing dry conditions that were caused by downslope water movement.

Combinations of higher landscape positions, shallow-moderate organic layer depths, and low soil moisture are more favourable for tree growth and, thus, these three classes were likely representative of reversible paludified areas in general. Field surveys showed that bedrock depressions were locally observed on these sloping surfaces (Fig. 6; for example, positions along transect 4 at 170 m to 240 m, 960 m to 990 m, and 1200 m to 1240 m). Occurrence of these depressions in the bedrock created locally wetter soil conditions that likely favoured local organic layer build-up (paludification). This finding is consistent with earlier studies where paludification occurred on sloping, well-drained terrain directly upon bedrock (Laamrani et al., 2013, 2014a; Payette, 2001; Simard et al., 2009), where humic material was negligible and fibric material dominates (Larocque et al., 2003). In most cases, these bedrock depressions could be identified from surface roughness of the bedrock, which was obtained from field data rather than on the basis of topographic position classification, because they did not correspond to depressions in the ground surface. To our knowledge, topographic maps of bedrock are not available; however, we have recently demonstrated the feasibility of using ground-penetrating radar (GPR) as a method for detecting and mapping local bedrock depressions beneath the organic layer (Laamrani et al., 2013).

3.4. Topographic Position Classification Performance

In this study, we used TPI values to semi-automatically derive topographic position classes (according to Weiss, 2001) from the

LiDAR-derived DTM. Indeed, we used quantitative landscape classification to differentiate between permanently and reversibly paludified forest soils. We also demonstrated that Weiss' classification method was a useful tool for classifying landscapes within flat to hilly areas of the Clay Belt. The initial classification divided the DTM into six topographic position classes, based on considerations of both local slope and landscape position, as measured by TPI. We revised this classification to increase recognisable sub-classes (based on slope and TWI information) that were assigned to one of the known paludification types. For example, the lower slope depression class was classified into closed and open depression sub-classes, which, respectively, represented permanent and reversible paludification types. Thus, cells in closed depressions were distinguished from cells that are not closed to downslope water movement. A suite of summary statistics describing the distribution of field data (OLT, fibric horizon thickness, tree basal area) within each topographic position class provided additional information that assists in assigning each class to a defined paludification type. This agrees with previous studies where factors other than morphological variables (e.g., vegetation, soil) were important considerations in defining topographic position classes and assigning them to ecological processes (Bou Kheir et al., 2010; MacMillan et al., 2007).

Overall, the classification that we used recognised major terrain features and effectively delimited major paludification patterns in the area. This was consistent with previous studies, which found that TPI offers a powerful approach for classifying the landscape into topographic classes, despite some restrictions (e.g., De Reu et al., 2013; Tagil and Jenness, 2008). However, occasional problems were experienced with Weiss' classification method: (i) areas around streams were classified as hilltops due to their elevated position relative to stream bottoms; thus, hilltops were most likely overrepresented. (ii) Subtle topographic differences within lower slope depressions and flat surfaces were not captured using the original classification. These problems might be dealt with by using more sensitive criteria such as modifying threshold breaking points of classes or assessing combinations of neighbourhood sizes.

3.5. Validation of the Resulting Maps

The assignment approach provided a set of decision rules that were applied in ArcGIS to create a thematic map of the resulting paludification types across the study area and for the entire LiDAR coverage area (~100 km^2). The map summarising the spatial distribution of permanent and reversible paludified areas is illustrated in Fig. 7. Validation of this map was based on a spatially continuous cross-sectional profile section of the surface topography that was generated along transect 4 (Fig. 6), and which was based on an independent field survey, consisting of 170 sampling points. Elevation values were extracted and used to generate the spatially continuous cross-sectional profile of the surface topography. Each sampling location along the profile was assigned to one of the six resulting topographic classes and compared to its corresponding class over the thematic map using a confusion matrix (matched-unmatched decisions). An overall 74% accuracy was achieved, suggesting that most permanent/reversible paludified sites could be accurately mapped. Flat surfaces had the highest match (87%), followed by lower slope depressions (86%). Hilltop, upper slopes and mid-slopes had the lowest matches (57%, 59%, and 62%, respectively), which may have been due to the prevalence of the aforementioned local depressions in the bedrock. Among sub-classes, flat bogs had the highest matches (96%). Open depression sites were accurately mapped (91% matching) compared to closed depression sites (80% matching).

3.6. Forest Management Implications and Paludification Type Assignment

From a management perspective, understanding the spatial distribution of topographic position classes is an important first step in predicting and mapping forest productivity across landscapes. TPI and

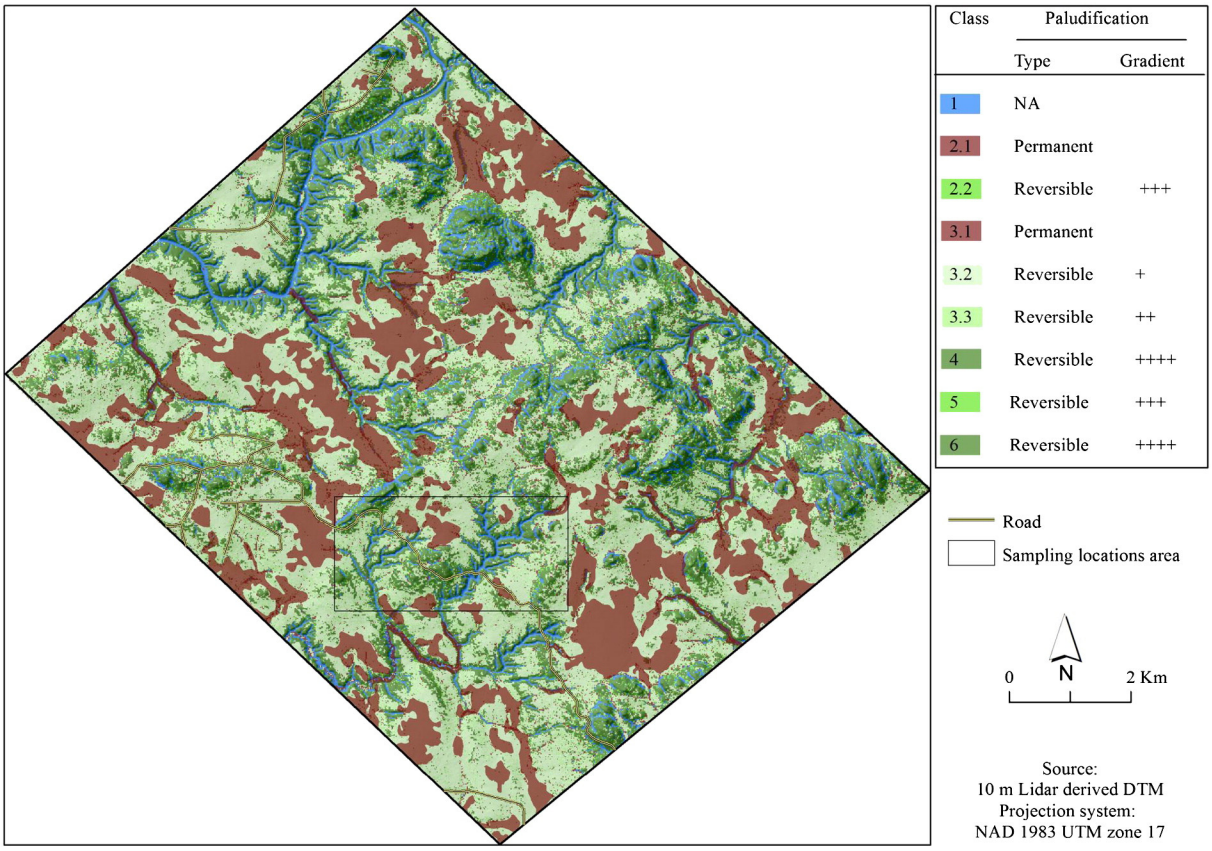

Fig. 7. Map showing the distribution of permanent and reversible paludified areas in the study area, and for the entire LiDAR coverage area (~100 km^2) within the Clay Belt.

TWI that are derived from remotely sensed LiDAR data are simple in concept to implement, easily defined, and provide intuitive notions of surface morphology and wetness. They can be used by forest managers to define promising areas for forest management and select sensitive areas where structure and biodiversity of paludified forest could be preserved; they can be used to map zones of saturation where organic layers are susceptible to accumulation; and landscapes can be classified into spatially homogenous units in terms of geomorphological and moisture characteristics. The method that we have employed offers a reasonable first approximation of a useful, stable framework for detecting and mapping permanent/reversible paludification in the Clay Belt (Table 2). It has the potential to facilitate forest management decisions, which in turn could improve forest productivity. For example, we demonstrated that (i) flat sites coinciding with mineral soil or bedrock depressions, and closed depression sites are very likely associated with deep organic layers and may reasonably be assigned to permanent paludification (Table 2). These areas are often not suitable for tree planting and provide no economic incentives for managing them; (ii) flat moderate/wet surfaces represent an advanced stage of paludification, but they might be reversed (Table 2) through mechanical site preparation (e.g., powered disc trenching), which would provide benefits through thick fibric layer removal; and (iii) mid-slopes, upper-slopes and hilltop sites and open depression sites represent early to moderate stages of reversible paludification (Table 2), which provides an important economic motive for managing them. Their low to moderate OLT and low moisture contents likely would not limit equipment that is used in mechanical site preparation and harvesting. However, the analytical approaches that we used have provided only a current snapshot of the paludified landscape, since paludification is a dynamic process that changes with time.

4. Conclusions

Our use of a semi-automated classification method for identifying morphological classes at the landscape scale has proven to be a promising technique for forest management. Together, TPI, slope and TWI identified continuous areas of the landscape that were linked to areas with varying wetness and morphological conditions, which could be used in mapping paludification types. About 74% of permanent/reversible paludified sites were accurately mapped, highlighting the suitability of the semi-automated approach for data exploration, and the mapping and differentiation of permanent/reversible paludification types. This method is easily implemented in ArcGIS, easy to understand, and thresholds can be modified or adapted when necessary, and could be applied to other boreal areas. It has the advantage of integrating topographic variables (e.g., slope) that in previous studies, have been found useful in explaining paludification types. This study also showed that splitting some initial classes into different sub-classes explained more variation in the spatial distribution of permanent/reversible paludified landscapes and provided more realistic relationships between topographic position classes, topographic indices, and field survey data. Unlike Weiss' topographic position-based spatial classes, our study benefited from the inclusion of field data on vegetation and soils to create classes with more comprehensive information on paludification. This study also demonstrated that LiDAR-derived DTM has great potential for forest management other than simply providing a set of elevation values, and yields a wide variety of landscape morphological characteristics, which may be important to forest managers and researchers in explaining and managing paludification. Finally, it should be mentioned that this study highlighted the role of bedrock in the spatial distribution of both paludification types on the landscapes of the Clay Belt and that more research is required on this issue.

Acknowledgements

The first author was financially supported by scholarships from the Fonds Québécois de la Recherche sur la Nature et les Technologies (FQRNT), the Natural Sciences and Engineering Research Council of Canada (NSERC), the NSERC-UQAT-UQAM Chair in Sustainable Forest Management, and Tembec Incorporated. Special thanks go to M. Louis Dumas (Tembec) for his valuable collaboration throughout the study, Dr. Benoît St. Onge from the Université du Quebec à Montréal (UQAM) for his help with the raw LiDAR data processing, and Dr. W.F.J. Parsons from the Centre d'étude de la forêt (CEF), who revised the English and helped to improve the quality of the manuscript. We also thank all the people who assisted us with the fieldwork. This research was funded by NSERC(# CRDPJ 390778 – 09)) and the Regional Conference of Elected Representatives of James Bay (# PPRMVF-2009-03), through the Programme de participation régionale à la mise en valeur des forêts-Quebec Ministry of Natural Resources. The authors are grateful to the editor and two anonymous reviewers for their constructive comments on an earlier version of this paper.

References

Beven, K.J., Kirkby, M.J., 1979. A physically based, variable contributing area model of basin hydrology. Hydrol. Sci. Bull. 24, 43–69.
Bou Kheir, R., Bøcher, P.K., Greve, M.B., Greve, M.H., 2010. The application of GIS based decision-tree models for generating the spatial distribution of hydromorphic organic landscapes in relation to digital terrain data. Hydrol. Earth Syst. Sci. 14, 847–857.
Clark, R.B., Creed, I.F., Sass, G.Z., 2009. Mapping hydrologically sensitive areas on the Boreal Plain: a multitemporal analysis of ERS synthetic aperture radar data. Int. J. Remote Sens. 30, 2619–2635.
Crawford, R.M.M., Jeffree, C.E., Rees, W.G., 2003. Paludification and forest retreat in northern oceanic environments. Ann. Bot.-Lond. 91, 213–226.
Creed, I.F., Beall, F.D., 2009. Distributed topographic indicators for predicting nitrogen export from headwater catchments. Water Resour. Res. 45, W10407.
Creed, I.F., Sass, G.Z., 2011. Digital terrain analysis approaches for tracking hydrological and biogeochemical pathways and processes in forested landscapes. In: Levia, D., Carlyle-Moses, D., Tanaka, T. (Eds.), Forest Hydrology and Biogeochemistry: Synthesis of Past Research and Future Directions. Springer-Verlag, New York, pp. 69–100.
De Reu, J., Bourgeois, J., Bats, M., Zwertvaegher, A., Gelorini, V., De Smedt, P., Chu, W., Antrop, M., De Maeyer, P., Finke, P., et al., 2013. Application of the topographic position index to heterogeneous landscapes. Geomorphology 186, 39–49.
Deumlich, D., Schmidt, R., Sommer, M., 2010. A multiscale soil–landform relationship in the glacial-drift area based on digital terrain analysis and soil attributes. J. Plant Nutr. Soil Sci. 173, 843–851.
Dormann, C.F., Elith, J., Bacher, S., Buchmann, C., Carl, G., Carré, G., Marquéz, J.R.G., Gruber, B., Lafourcade, B., Leitão, P.J., et al., 2013. Collinearity: a review of methods to deal with it and a simulation study evaluating their performance. Ecography 36, 027–046.
Emili, L.A., Price, J.S., Fitzgerald, D.F., 2006. Hydrogeological influences on forest community type along forest–peatland complexes in coastal British Columbia. Can. J. For. Res. 36, 2024–2037.
Environment Canada, 2011. Canadian Climate Normals 1971–2000. Matagami Weather Station. Available online at http://climate.weather.gc.ca/climate_normals/ (Last accessed April 2014).
ESRI, 2011. ArcGIS Desktop: Release 10. Environmental Systems Research Institute, Redlands, CA, USA. Available online at http://help.arcgis.com/en/arcgisdesktop/10.0/help/ (last accessed January 2014).
Fenton, N.J., Bergeron, Y., 2006. Facilitative succession in a boreal bryophyte community driven by changes in available moisture and light. J. Veg. Sci. 17, 65–76.
Fenton, N., Lecomte, N., Légaré, S., Bergeron, Y., 2005. Paludification in black spruce (*Picea mariana*) forests of eastern Canada: potential factors and management implications. For. Ecol. Manag. 213, 151–159.
Fenton, N.J., Simard, M., Bergeron, Y., 2009. Emulating natural disturbances: the role of silviculture in creating even-aged and complex structures in the black spruce boreal forest of eastern North America. J. For. Res. 14, 258–267.
Gorozhankina, S.M., 1997. Paludification in the Tsentral'no-Sibirskii Biosphere Reserve (the Yenisei region of Siberia). Russ. J. Ecol. 28, 67–72.
Jenness, J., Majka, D., Beier, P., 2011. Corridor Designer Evaluation Tools: Extension for ArcGIS. Jenness Enterprises, Flagstaff, AZ, USA, (Available at: http://www.jennessent.com/arcgis/corridor.htm. Last accessed January 2014).
Laamrani, A., Valeria, O., Cheng, L.-Z., Yves Bergeron, Y., Camerlynck, C., 2013. The use of ground penetrating radar for remote sensing the organic layer–mineral soil interface in paludified boreal forests. Can. J. Remote. Sens. 39, 74–88.
Laamrani, A., Valeria, O., Fenton, N., Bergeron, Y., 2014a. Landscape—scale influence of topography on organic layer accumulation in paludified boreal forests. For. Sci. 60, 579–590. http://dx.doi.org/10.5849/forsci.13-025 (Available online).
Laamrani, A., Valeria, O., Fenton, N., Bergeron, Y., Cheng, L.Z., 2014b. The role of mineral soil topography on the spatial distribution of organic layer thickness in a paludified boreal landscape. Geoderma 221–222, 70–78. http://dx.doi.org/10.1016/j.geoderma.2014.01.003.
Laamrani, A., Valeria, O., Fenton, N., Bergeron, Y., Cheng, L.Z., 2014c. Effects of topography and thickness of organic layer on productivity of black spruce boreal forests of the Canadian Clay Belt region. For. Ecol. Manag. 330, 144–157. http://dx.doi.org/10.1016/j.foreco.2014.07.013.

Larocque, I., Bergeron, Y., Campbell, I.D., Bradshaw, R.H.W., 2003. Fire-induced decrease in forest cover on a small rock outcrop in the Abitibi region of Québec, Canada. Ecoscience 10, 515–524.
Lavoie, M., Pare, D., Fenton, N., Groot, A., Taylor, K., 2005. Paludification and management of forested peatlands in Canada: a literature review. Environ. Rev. 13, 21–50.
Lavoie, M., Harper, K., Paré, D., Bergeron, Y., 2007. Spatial pattern in the organic layer and tree growth: a case study from regenerating *Picea mariana* stands prone to paludification. J. Veg. Sci. 18, 213–222.
Lindsay, J.B., Creed, I.F., 2005. Removal of artifact depressions from digital elevation models: towards a minimum impact approach. Hydrol. Process. 19, 3113–3126.
MacMillan, R.A., Moon, D.E., Coupé, R.A., 2007. Automated predictive ecological mapping in a forest region of BC, Canada, 2001–2005. Geoderma 140, 353–373.
McKenzie, N.J., Ryan, P.J., 1999. Spatial prediction of topsoil properties using environmental correlation. Geoderma 89, 67–94.
Moore, I.D., Lewis, A., Gallant, J.C., 1993. Terrain attributes: estimation methods and scale effects. In: Jakeman, A.J., Beck, M.B., McAleer, M.J. (Eds.), Modelling Change in Environmental Systems. Wiley, London, pp. 189–214.
Payette, S., 2001. Les principaux types de tourbières. In: Payette, S., Rochefort, L. (Eds.), Écologie des tourbières du Québec-Labrador: une perspective nord-américaine. Presses de l'Université Laval, Québec, QC, pp. 39–89.
R Development Core Team, 2011. R: A Language and Environment for Statistical Computing. R Foundation for Statistical Computing, Vienna, Austria, (URL http://www.R-project.org/).
Robitaille, A., Saucier, J.-P., 1998. Paysages régionaux du Québec méridional. Les publications du Québec, Québec, (213 pp.).
Simard, M., Lecomte, N., Bergeron, Y., Bernier, P.Y., Paré, D., 2007. Forest productivity decline caused by successional paludification of boreal soils. Ecol. Appl. 17, 1619–1637.
Simard, M., Bernier, P.Y., Bergeron, Y., Paré, D., Guérine, L., 2009. Paludification dynamics in the boreal forest of the James Bay Lowlands: effect of time since fire and topography. Can. J. For. Res. 39, 546–552.
Sørensen, R., Zinko, U., Seibert, J., 2006. On the calculation of the topographic wetness index: evaluation of different methods based on field observations. Hydrol. Earth Syst. Sci. 10, 101–112.
Southee, F.M., Treitz, P.M., Scott, N.A., 2012. Application of LiDAR terrain surfaces for soil moisture modelling. Photogramm. Eng. Remote Sens. 78, 1241–1251.
Tagil, S., Jenness, J.S., 2008. GIS-based automated landform classification and topographic, landcover and geologic attributes of landforms around the Yazoren Polje, Turkey. J. Appl. Sci. 8, 910–921.
Tchir, T.L., Johnson, E.A., Miyanishi, K., 2004. A model of fragmentation in the Canadian boreal forest. Can. J. For. Res. 34, 2248–2262.
Veillette, J.J., 1994. Evolution and paleohydrology of glacial Lakes Barlow and Ojibway. Quat. Sci. Rev. 13, 945–971.
Weiss, A.D., 2001. Topographic positions and landforms analysis (Conference Poster). ESRI International User Conference, San Diego, CAIndus Corporation, Seattle, WA.
Wilson, J.P., Gallant, J.C., 2000. Secondary topographic attributes. In: Wilson, J.P., Gallant, J.C. (Eds.), Terrain Analysis: Principles and Applications. Wiley, New York, pp. 87–131.